Ferromagnetic and Electrical Characteristics of in Situ Manganese-Doped GaN Nanowires

Congkang Xu,[†] Junghwan Chun,[†] Hyo Jin Lee,[†] Yoon Hee Jeong,[†] Seong-Eok Han,[‡] Ju-Jin Kim,[‡] and Dong Eon Kim*,[†]

Department of Physics and Electron Spin Science Center, Pohang University of Science and Technology, Pohang 790-784, Korea, and Department of Physics, Chonbuk National University, Jeonju 561-756, Korea

Received: August 19, 2006; In Final Form: October 27, 2006

The ferromagnetic and electrical characteristics of in situ Mn-doped GaN nanowires fabricated in the absence of any catalyst are reported. The nanowires are of single-crystal hexagonal structure, containing Mn up to 2.5 atom %. Magnetism measurements indicate that the nanowires have room temperature ferromagnetism with Curie temperature above 350 K. Magnetic force microscopy verifies that the ferromagnetism of the individual nanowire is uniform along the nanowire. An electrical transport measurement reveals that the nanowire has a weak gating effect and is of the n-type.

1. Introduction

Adding guest atoms to inorganic nanotubes, known as doping, influences their room temperature magnetic properties that can be exploited in spintronic devices.[1,2] Dilute magnetic semiconductor (DMS) nanostructures having a high Curie temperature (T_c) are of intense interest in the research community given their implications for the design of spintronic nanodevices[3] such as electronic-optic switches, ultrasensitive magnetic field sensors, magnetic hard disk media, spin field effect transistors (FETs), resonant tunneling diodes (RTDs), and nonvolatile computer memory chips.[4−6] Prompted by the high-Tc DMS prediction for a p-type GaN of 5% Mn concentration,[7,8] numerous studies on DMS-based GaN bulks and films have been conducted.[9−15] In essence, GaN exhibits n-type behavior because of nitrogen vacancies and/or oxygen impurities.[16] It would also be highly desirable if an n-type DMS with a T_c in excess of 300 K could be achieved, because the performance of devices such as RTDs should be better for n-type conduction. In another sense, the ongoing trend toward the miniaturization of electronic devices enables one to foresee highly potential applications of one-dimensional (1D) nanostructures, such as nanowires and nanotubes being utilized as possible building blocks for next-generation electronic devices. One-dimensional ferromagnetic semiconductor nanostructures, suitable for controlled fabrication and magnetic doping, are cutting-edge in the development of spin-based multifunctional devices as well as for the understanding of fundamental properties. In addition, the availability of single-crystalline DMS nanostructures is of significance for scrutinizing the evolution of ferromagnetism by suppressing extrinsic effects such as secondary phases. Mn-doped GaN 1D nanostructures are expected to be one of the most promising candidates to fulfill these requirements. Although progress has been made in the fabrication and characterization of Mn-doped and Mn/Al-codoped GaN nanowires,[17−20] the origin of room temperature ferromagnetism, which possibly arises from magnetic impurities or phase-separation, is still a matter of controversy. To address the contentious issues of DMS nitride phases, including the questions of nanocrystalline ferro (ferri) magnetic impurities such as GaMn and Mn_4N, we herein aim at the fabrication of high-purity in situ Mn-doped single-crystal GaN nanowires via a simple vapor phase transport method without catalyst, template mediation, or codoping. The high purity of the samples was ensured, since they were produced in bulk quantity by a simple, one-step and in situ doping process without any metal catalyst. We also investigated the room temperature ferromagnetism and current−voltage characteristics of the GaN:Mn nanowires.

2. Fabrication

An alumina boat containing a mixture of GaN powder (Aldrich, 99.99%) with manganese acetylacetonate ($Mn(C_5H_7O_2)_3$, Aldrich, 99.99%) was located in the center of a quartz tube placed horizontally in a tubular furnace. A sapphire substrate was placed 300 mm downstream from the boat. The base vacuum was kept at 95 mTorr. The powder was heated to 900 °C at a rate of 20 °C/min with a flow of Ar 95% + H_2 5% at 80 SCCM (standard cubic centimeters per minute). Ammonia gas (99.999%) was introduced at 150 SCCM after the Ar + H_2 gas was turned off. The system was then heated at a rate of 10 °C to ∼1080 °C for 300 min, and the pressure was maintained at 500 Torr. After the system was cooled with NH_3, the wool-like light-yellow-colored products were removed from the sapphire substrate. In order to gain further insights into the ferromagnetic and electrical properties of the Mn-doped GaN nanowires, undoped GaN nanowires had been prepared under identical conditions but without manganese acetylacetonate.

A structure analysis was conducted using scanning electron microscopy (SEM, Hitachi S-4300 SE), X-ray diffraction (XRD, Japanese Rigaku), and field emission transmission electron microscopy (TEM, JEOL-2010) equipped with energy-disperse X-ray fluorescence (EDX). The magnetic properties were determined using a superconducting quantum interference device (SQUID) magnetometer and magnetic force microscopy (MFM). A two-terminal technique was employed to measure the electrical characteristics.

3. Measurement and Discussion

Figure 1 shows the SEM images of the as-obtained samples grown on the sapphire substrate. A bulk quantity of nanowires

* Corresponding author. E-mail: kimd@postech.ac.kr.
[†] Pohang University of Science and Technology.
[‡] Chonbuk National University.

10.1021/jp065378j CCC: $37.00 © 2007 American Chemical Society
Published on Web 12/14/2006

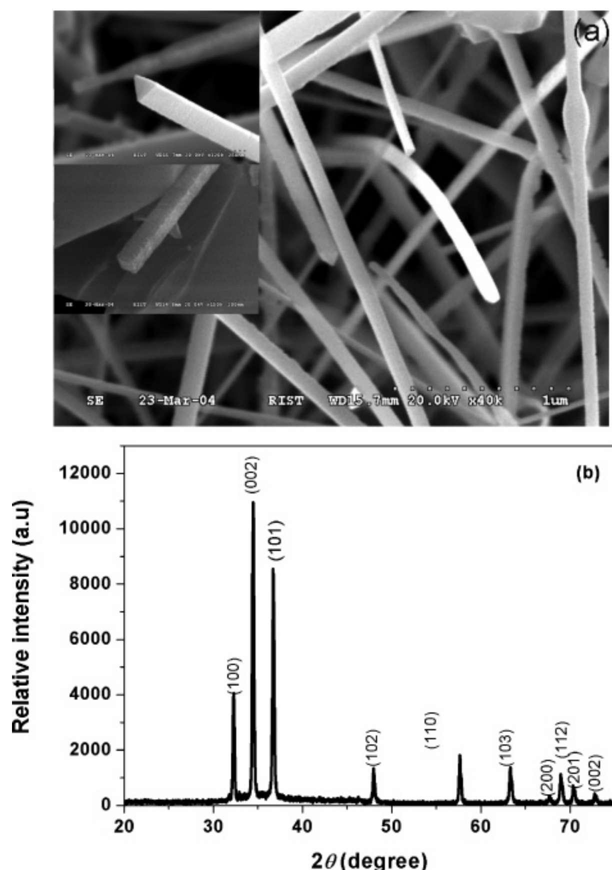

Figure 1. (a) SEM images of GaMnN nanowires. The insets are two nanowires of triangular and square cross-section, respectively. (b) XRD pattern of GaMnN nanowires.

is distributed over the entire surface of the substrate. The average diameter of the nanowires is around 80 nm, and the length is up to a few micrometers. A significant fraction of nanowires exhibits a triangular cross-section (the upper inset). A minor fraction of nanowires is of square cross-section (the lower inset) or cylindrical. The surfaces of the nanowires are smooth and clean. The crystal structures of the nanowires were determined by XRD. The diffraction peaks (Figure 1b) fully correspond to those of bulk GaN of hexagonal wurtzite structure ($a = 3.095$ Å, $c = 5.00$ Å) (ICSD# 067769). No typical diffraction peaks corresponding to Mn or Mn-compound phases such as GaMn and Mn_4N are observed.

Figure 2a shows the TEM image and TEM-based EDX of a nanowire of ~100 nm diameter. The EDX analysis (the lower inset) indicates that the nanowire is composed of Ga, Mn, and N, with an atomic ratio of 52:1:47. The atomic ratio of Ga to Mn is about 98:2, and the observed Cu element is probably due to the TEM grid. Different areas of an individual nanowire and dozens of nanowires were examined by TEM-based EDX. Statistical analyses of these data indicate that the Mn content for all areas of the nanowire is nearly homogeneous, and for different nanowires ranges from 1.55 to 1.75 atom %. The selected area electron diffraction (SAED) (the upper inset) does not show any 4-fold symmetry pattern, which would be present if either tetragonal or cubic phases such as GaMn and Mn_4N were formed in the nanowires. The SAED also reveals that the nanowire is a single crystal of hexagonal structure and grows in the [001] direction, indicating that the GaN:Mn nanowires have the same lattice structure as bulk GaN. Figure 2b shows a typical high-resolution TEM image of the corresponding nanowire. The clear fringes perpendicular to the long axis of

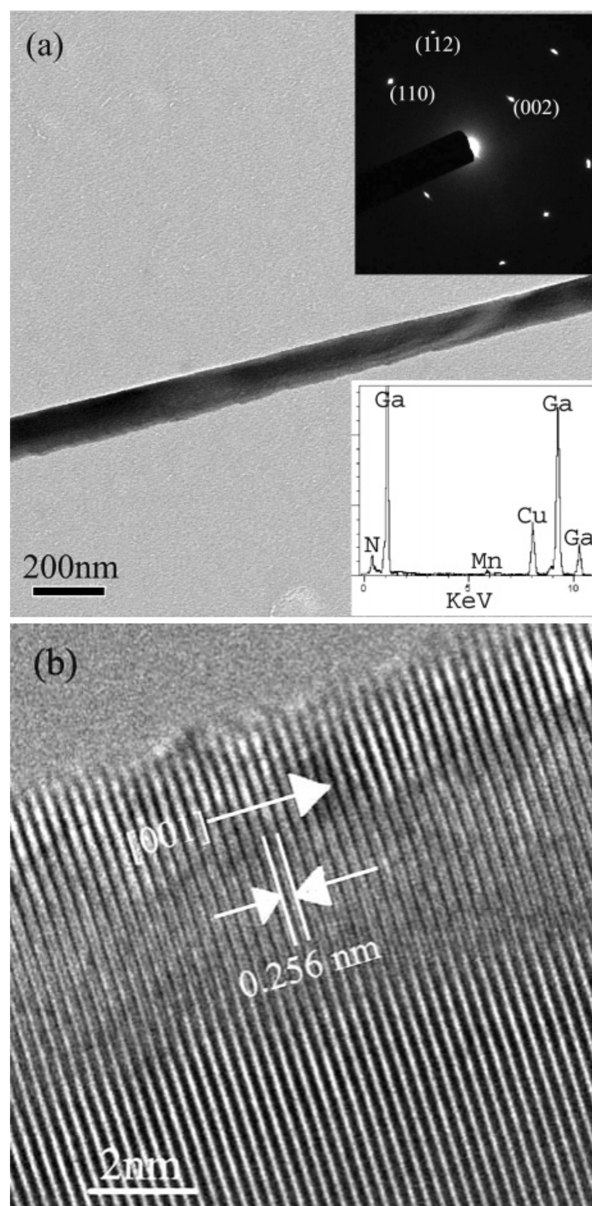

Figure 2. TEM image of nanowire. (a) TEM image of nanowire of ~100 nm diameter. The upper inset is the selected area electron diffraction pattern and the lower inset, the EDX. The observed Cu element is probably due to the TEM grid. (b) An HRTEM image of a nanowire.

the nanowire with a spacing of 0.256 nm correspond to the (002) plane of hexagonal GaN, further indicating that the single-crystalline nature of the nanowire is without secondary phase inclusions or clusters.

Additional experiments varying the weight ratio of manganese acetylacetonate and GaN showed that the Mn content was not larger than 2.5 atom %, and no traces of secondary phases were detected by XRD, EDX, or HRTEM. These results are in accord with those of previous report on molecular beam epitaxy (MBE)-grown Mn-doped GaN film,[21] where the maximum solubility of Mn in a GaN film without a secondary phase was shown to be less than 3 atom %. While most Mn-doped DMSs fabricated by MBE and implantation or catalyst-assisted processes suffered from secondary phase or contamination, the GaN:Mn nanowires reported here prepared by a simple, one-step, catalyst-free, and in situ-doped process are single-crystalline without phase separation or clusters. More importantly, there are no catalysts used here, such as Fe, Co, and Ni, which might affect

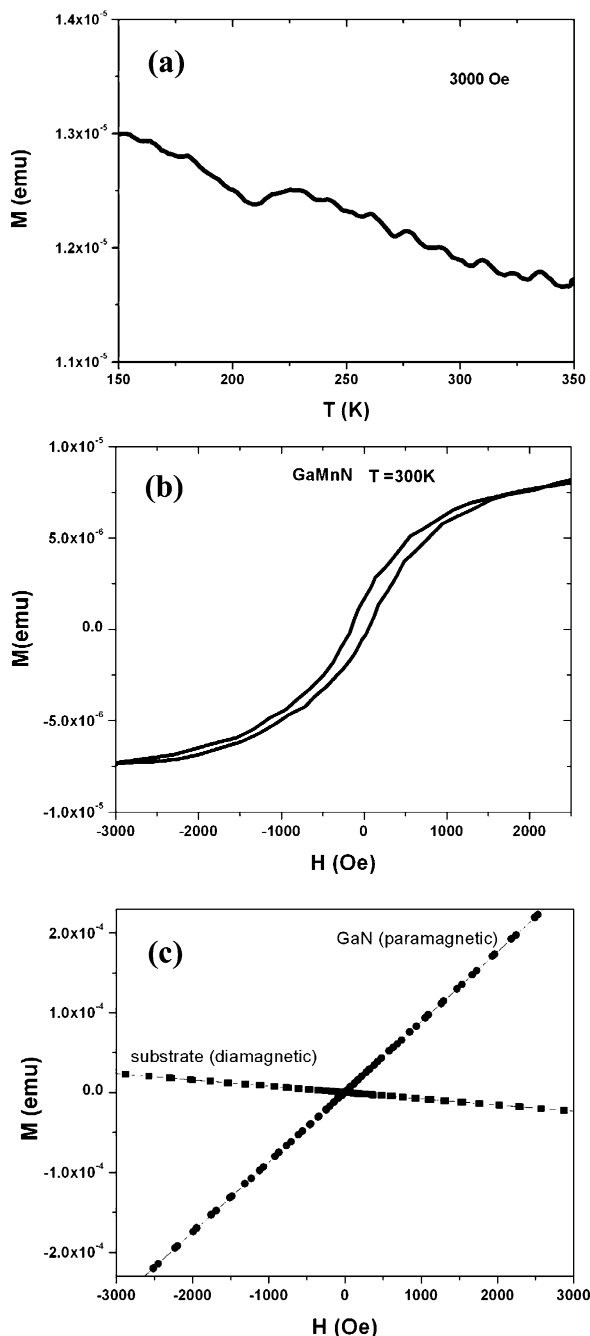

Figure 3. (a) $M-T$ of GaMnN nanowires. (b) $M-H$ of GaMnN nanowires. (c) $M-H$ behavior of sapphire substrate (diamagnetic) and undoped GaN nanowires (paramagnetic) at 300 K.

exploration of the origin of ferromagnetism. The high purity of the samples is thus ensured.

The magnetic properties of the as-grown Mn-doped GaN nanowires were measured by a SQUID magnetometer. A typical magnetic moment (M) versus temperature (T) curve was measured during cooling under an applied magnetic field of 3000 Oe. Figure 3a shows the $M-T$ of the GaMnN nanowires, where the T_c is at, at least, 350 K. Figure 3b shows the field dependence of magnetic moment ($M-H$) curve of the GaMnN nanowires at 300 K. A hysteretic loop is observed to show ferromagnetic properties of coercivity (H_c) and remanent magnetic moment (M_r), 100 Oe and 1.5×10^{-6} emu, respectively. The origin of ferromagnetism in transition-metal-doped semiconductors has been controversial because of the possible presence of ferromagnetic transition metal or metal nitride particles. The absence of any detectable traces of secondary phases or clusters in the EDX and HRTEM clearly excludes the possibility of the presence of ferromagnetic GaMn and Mn_4N. Ferromagnetic behavior can also be observed if the nanowires are contaminated with magnetic impurities, such as Fe, Ni, or Co, by improper handling or from source contamination. We found by measuring undoped GaN nanowires fabricated under identical conditions to those for GaN:Mn nanowires that these undoped GaN nanowires show no ferromagnetism except paramagnetism (Figure 3c) at room temperature. The fact that the paramagnetic response from undoped GaN nanowires appears to be 100 times larger than the ferromagnetic response from GaN:Mn nanowres is due to the volume of the sample. By doing so, we rule out the possibility of error in the measurement equipment itself and diamagnetic sapphire substrate (Figure 3c) as well as magnetic impurities such as Fe, Ni, and Co from starting materials, because the GaN and Mn($C_5H_7O_2$)$_3$ powders were of 99.99% purity.

MFM offers a powerful technique for checking the distribution of ferromagnetism, whether uniform or local. Figures 4a and b show a topographical image of a 11.4×11.4 μm^2 area taken under atomic force microscopy (AFM) as well as the corresponding MFM image, respectively. The topographical image confirms that the nanowire is of ~100 nm diameter and ~10 μm length. The MFM image comes from the magnetic response instead of the surface effects. The absence of a clear contrast on the nanowire's surface indicates that it is a highly homogeneous nanowire without any clusters or domains. In order to exclude the crosstalk between the topographical signal (AFM) and the magnetic signal (MFM), we performed a comparative measurement of nonmagnetic ZnO nanowires of similar dimensions using MFM. A topographical image taken of a 10×10 μm^2 area is shown in Figure 4c. No magnetic signal was observed from the corresponding MFM image (Figure 4d). These findings indicate that the detected signal from Figure 4b was not due to the crosstalk.

To identify the electrical properties of GaN:Mn nanowires, a series of current versus voltage ($I-V$) measurements were performed. Electrical contacts were made to a single nanowire as follows. Alignment marks consisting of a metal dot array with about 1 μm spacing were fabricated on a heavily doped Si substrate with a 300 nm thermally grown SiO_2 layer which acts as the global back-gate.[23] A droplet of dispersed enthanol solution containing nanowires was dropped onto the substrate. Once the solution was blown dry, some nanowires were fixed on the surface. A suitable nanowire was selected via SEM. Once the nanowire was found, its position was determined relative to the alignment marks. A two-layer e-beam resist (PMMA/copolymer) was then spun over the sample, and the patterns for the electrical leads were generated, using e-beam lithography techniques, onto the pre-selected nanowire. Then Ti (~150 nm) and Au (~50 nm) were sequentially deposited onto the contact area by thermal evaporation. The electrodes were formed by a subsequent lift-off process. As shown in Figure 5, the two-terminal electrical resistance R for undoped GaN and Mn-doped GaN nanowires was measured as a function of temperature in an He-3 system down to 50 K. Figure 5a shows the temperature-dependent electrical resistance $R(T)$ of an undoped GaN nanowire. The resistance consistently increased monotonically as the temperatures decreased, revealing the typical characteristics of a semiconductor. No anomaly was observed. Figure 5b shows the temperature-dependent electrical resistance $R(T)$ of an Mn-doped GaN nanowire. The resistance did not always increase as the temperature decreased from 325 to 50 K; rather,

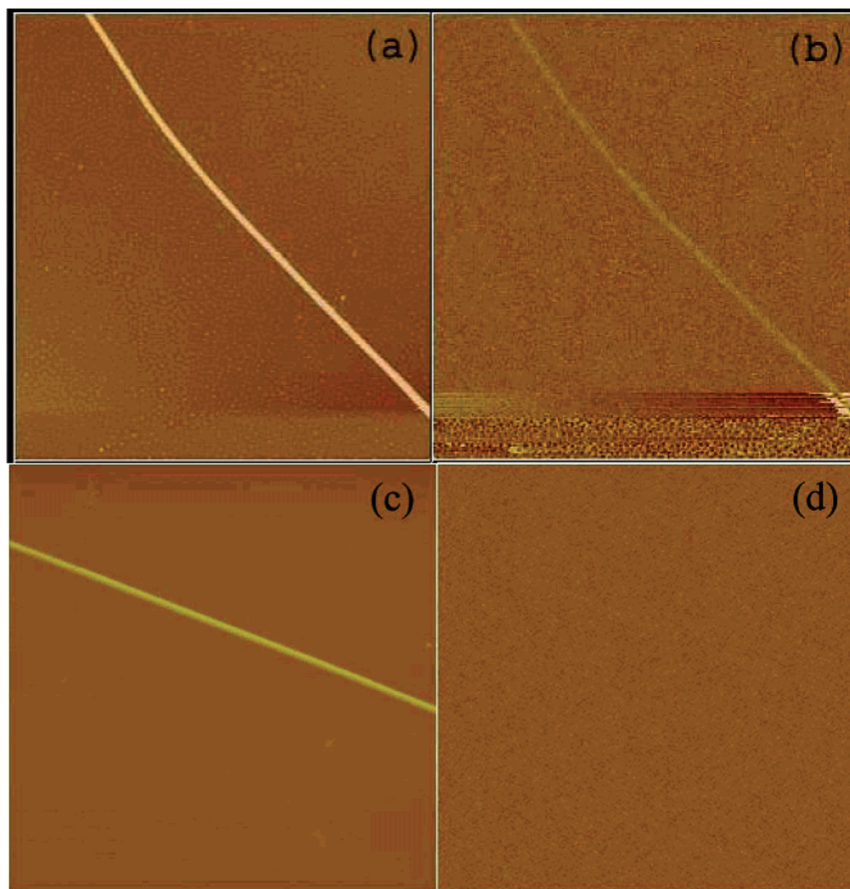

Figure 4. AFM (a) and MFM (b) images of individual Mn-doped GaN nanowire taken at room temperature for 11.4 × 11.4 μm^2 area. AFM (c) and MFM (d) images of an individual nonmagnetic ZnO nanowire taken at room temperature for a 10 × 10 μm^2 area. The tip was applied perpendicular to the nanowire's surface.

the resistance decreased with decreasing temperatures from 325 to 210 K, and then increased as the temperature further decreased, demonstrating that it is not an inherent material property of GaN. The resistivity response of GaN:Mn nanowires shows that it goes through a metal insulator transition, the dip in the curve being located at ~210 K. This phenomenon is probably due to the critical scattering.[22]

Figures 6a and b show typical current versus source-drain voltage ($I-V_{ds}$) data at different gate voltages (V_g) as well as the transport characteristics $I-V_g$ at different source-drain voltages (V_{ds}), obtained from an undoped GaN nanowire FET. The two-terminal $I-V_{ds}$ curves (Figure 6a) exhibit a linear response, thus indicating that the contacts behave, in a practical sense, as ohmic. For a given V_{ds}, I increases with increasing positive V_g: that is, the conductance of the nanowire increases with increasing positive gate voltage V_g. This clearly indicates that the GaN:Mn nanowires are of the n-type. The gate response $I-V_g$ curves (Figure 6b) also show that the undoped GaN nanowire is of the n-type; that is, the conductance of the nanowires increases with increasing positive V_g. The change in current is more than 38 nA by varying the gate voltage from −10 to +10 V (V_{ds} = 4 mV). According to previous studies of bulk materials, the n-type characteristics of undoped GaN nanowires could be attributed to nitrogen vacancies and/or oxygen impurities.[16] Panels c and d of Figure 6 reveal the $I-V_{ds}$ data and $I-V_g$ curve obtained from a single Mn-doped GaN nanowire FET. The two-terminal $I-V_{ds}$ curve is also linear (enlarged in the inset), manifesting the fact that the metal electrodes make good ohmic contacts to the Mn-doped GaN nanowire. For a given V_{ds}, I increased with increasing positive V_g, indicating that the doped GaN was of the n-type. As seen

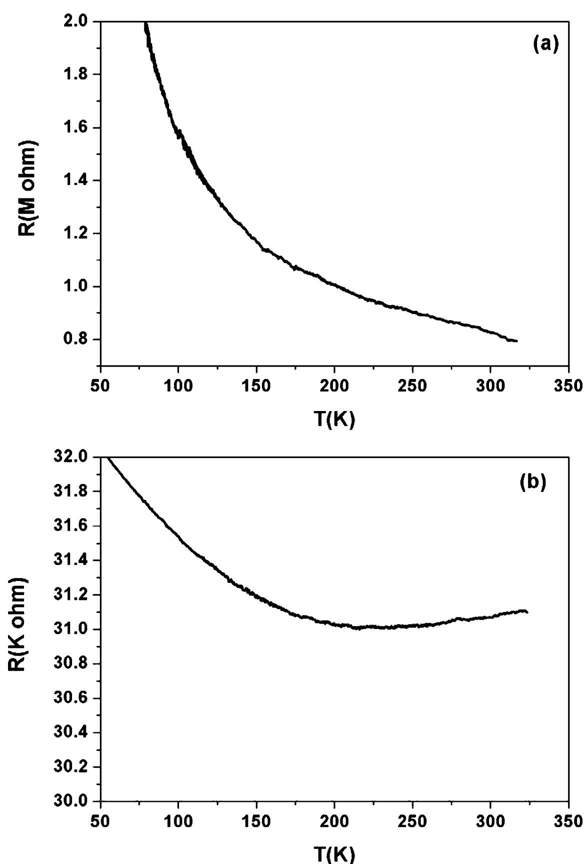

Figure 5. (a) Temperature-dependent electrical resistance $R(T)$ of undoped GaN nanowire. (b) $R-T$ curve of Mn-doped GaN nanowire.

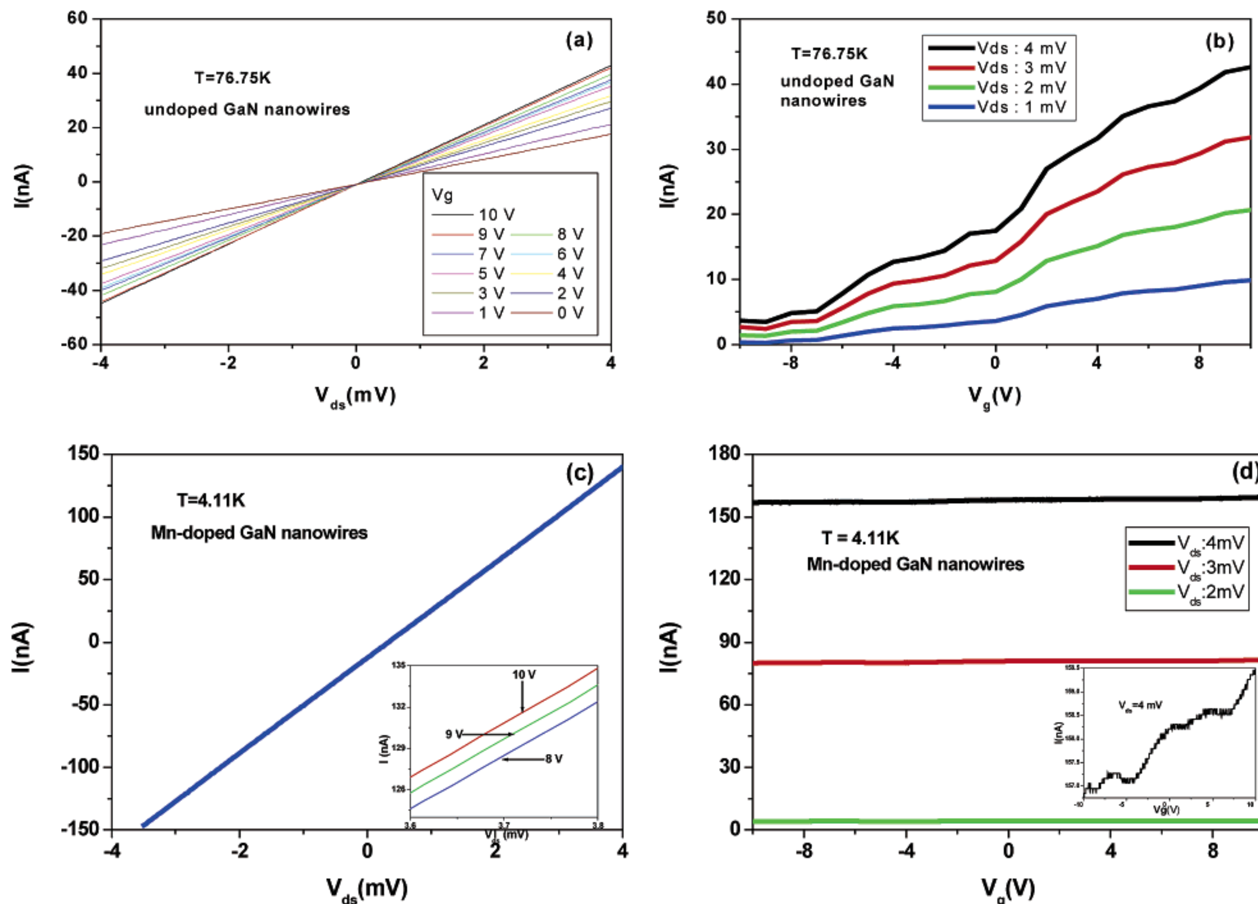

Figure 6. (a) Current versus source-drain voltage ($I-V_{ds}$) at different gate voltages (V_g) and (b) transport characteristics $I-V_g$ at different source-drain voltages of individual undoped GaN nanowire. (c) $I-V_{ds}$ of single Mn-doped GaN nanowire, and inset is enlarged $I-V_{ds}$ with V_g =10, 9, 8 V. (d) $I-V_g$ curve of single Mn-doped GaN nanowire, and inset is enlarged $I-V_g$ at V_{ds} = 4 mV.

from the $I-V_g$ curve (Figure 6d), the change in current (the inset) is less than 3 nA by changing the gate voltage from −10 to +10 V (V_{ds} = 4 mV). This finding shows that Mn-doped GaN nanowire has a weak gating effect as compared with undoped GaN nanowire. In fact, n-type GaMnN films exhibiting room temperature ferromagnetism have already been observed.[15,24] From the mean-field theory point of view, it is not feasible to attain high T_c in n-type materials. This discrepancy might be due to the hydrogen incorporation and/or nitrogen vacancy that might make the crystal field attained in this study different from the one in ideal GaN.

4. Conclusions

In summary, the ferromagnetic and electrical characteristics of in situ Mn-doped GaN nanowires are reported. The nanowires are of single-crystal hexagonal structure, Mn-doped to 1.5−2 atom %. SQUID results show that the nanowires have room temperature ferromagnetism with T_c above 350 K. MFM clearly verifies that the ferromagnetism of the individual nanowire is uniform instead of local. The determination of the $I-V$ electrical characteristics reveals that the nanowire has a weak gating-effect and is of the n-type.

Acknowledgment. This work was partially supported by the electron Spin Science Center eSSC and a National Research Laboratory (NRL) project, funded by the Korean Science and Engineering Foundation (KOSEF), and by Brain Korea (BK) 21, funded by the Korea Research Foundation.

References and Notes

(1) Tenne, R. R. *Nature* **2004**, *431*, 640.

(2) Krusin-Elbaum, L.; Newns, D. M.; Zeng, H.; Derycke, V.; Sun, J. Z.; Sandstrom, R. *Nature* **2004**, *431*, 672.

(3) Datta, S.; Das, B. *Appl. Phys. Lett.* **1990**, *56*, 665.

(4) Divincenzo, D. *Science* **1995**, *270*, 225.

(5) Prinz, G. A. *Science* **1998**, *282*, 1660.

(6) Awschalom, D. D.; Kawakami, P. K. *Nature* **2000**, *408*, 923.

(7) Dietl, T.; Ohno, H.; Matsukura, F.; Cibert, J.; Ferrand, D. *Science* **2000**, *287*, 1019.

(8) Sato, K.; Yoshida, H. K. *Jpn. J. Appl. Phys.* **2001**, *40*, L485.

(9) Soo, Y. L.; Kioseoglou, G.; Kim, S.; Huang, S.; Kao, Y. H.; Kumabara, S.; Owa, S.; Kondo, T.; Munekata, H. *Appl. Phys. Lett.* **2001**, *79*, 3926.

(10) Shon, Y.; Kwon, Y. H.; Kim, D. Y.; Fan, X.; Fu, D.; Kang, T. W. *Jpn. J. Appl. Phys.* **2001**, *40*, L5304.

(11) Kuwabara, S.; Kondo, T.; Chikyow, T.; Ahmet, P.; Munekata, H. *Jpn. J. Appl. Phys.* **2001**, *40*, L724.

(12) Sonada, S.; Shimizu, S.; Sasaki, T.; Yamamoto, Y.; Hori, H. *J. Cryst. Growth* **2002**, *237/239*, 1358.

(13) Zajac, M.; Doradzinski, R.; Gosk, J.; Szczytko, J.; Lefeld-Sosnowska, M.; Kaminska, M.; Twardowski, A.; Palczewska, M.; Grzanka, E.; Gebicki, W. *Appl. Phys. Lett.* **2001**, *78*, 1276.

(14) Theodoropoulou, N.; Hebard, A. F.; Overberg, M. E.; Abernathy, C. R.; Pearton, S. J.; Chu, S. N. G.; Wilson, R. G. *Appl. Phys. Lett.* **2001**, *78*, 3475.

(15) Reed, M. L.; El-Masry, N. A.; Stadelmaier, H. H.; Ritums, M. K.; Reed, M. J.; Parker, C. A.; Roberts, J. C.; Bedair, S. M. *Appl. Phys. Lett.* **2001**, *79*, 3473.

(16) Huang, Y.; Duan, X.; Cui, Y.; Lieber, C. M. *Nanolett.* **2002**, *2*, 101.

(17) Han, D.; Park, J.; Rhie, K.; Kim, S.; Chang, J. *Appl. Phys. Lett.* **2005**, *86*, 032506.

(18) Choi, H.; Seong, H.; Chang, J.; Lee, K.; Park, Y.; Kim, J.; Lee, S.; He, R.; Kuykendall, T.; Yang, P. *Adv. Mater.* **2005**, *17*, 1351.

(19) Xu, C. K.; Chun, J.; Rho, K.; Kim, D. E.; Kim, B. J.; Yoon, S.; Han, S. E.; Kim, J. J. *J. Appl. Phys.* **2006**, *99*, 064312.

(20) Deepak, F. L.; Vanitha, P. V.; Govindaraj, A.; Rao, C. N. R. *Chem. Phys. Lett.* **2003**, *374*, 314.

(21) Thaler, G.; Frazier, R.; Gila, B.; Stapleton, J.; Davidson, M.; Abernathy, C. R.; Pearton, S. J.; Segre, C. *Appl. Phys. Lett.* **2004**, *84*, 1314.

(22) Matsukura, F.; Ohno, H.; Shen, A.; Sugawara, Y. *Phys Rev. B.* **1998**, *57*, R2037.

(23) Huang, Y.; Duan, X.; Cui, Y.; Lauhon, L. J.; Kim, K.; Lieber, C. M. *Science* **2001**, *294*, 1313.

(24) Thaler, G. T.; Overberg, M. E.; Gila, B.; Frazier, R.; Abernathy, C. R.; Pearton, S. J.; Lee, J. S.; Lee, S. Y.; Park, Y. D.; Kim, Z. G.; Kim, J.; Ren, F. *Appl. Phys. Lett.* **2002**, *80*, 3964.